HHS Public Access

Author manuscript

Stroke. Author manuscript; available in PMC 2018 March 01.

Published in final edited form as:

Stroke. 2017 March ; 48(3): 754–761. doi:10.1161/STROKEAHA.116.015878.

The Role of Genetic Variation in Collateral Circulation in the Evolution of Acute Stroke: A Multimodal MRI Study

Yu-Chieh Jill Kao, PhD[1,2,3,4,*], **Esteban A. Oyarzabal, MS**[1,2,5,*], **Hua Zhang, MD**[6,7], **James E Faber, PhD**[5,6,7], and **Yen-Yu Ian Shih, PhD**[1,2,7,8]

[1]Department of Neurology, University of North Carolina, Chapel Hill, NC, USA

[2]Biomedical Research Imaging Center, University of North Carolina, Chapel Hill, NC, USA

[3]Translational Imaging Research Center, College of Medicine, Taipei Medical University, Taipei, Taiwan

[4]Department of Radiology, School of Medicine, College of Medicine, Taipei Medical University, Taipei, Taiwan

[5]Neurobiology Curriculum, University of North Carolina, Chapel Hill, NC, USA

[6]Department of Cell Biology and Physiology, University of North Carolina, Chapel Hill, NC, USA

[7]McAllister Heart Institute, University of North Carolina, Chapel Hill, NC, USA

[8]Department of Biomedical Engineering, University of North Carolina, Chapel Hill, NC, USA

Abstract

Background and Purpose—No studies have determined the effect of differences in pial collateral extent (number and diameter), independent of differences in environmental factors and unknown genetic factors, on severity of stroke. We examined ischemic tissue evolution during acute stroke, as measured by magnetic resonance imaging (MRI) and histology, by comparing 2 congenic (CNG) mouse strains with otherwise identical genetic backgrounds but with different alleles of the *Determinant of collateral extent-1* (*Dce1*) genetic locus. We also optimized magnetic resonance (MR) perfusion and diffusion deficit thresholds by using histological measures of ischemic tissue.

Methods—Perfusion, diffusion, and T_2-weighted MRI were performed on collateral-poor (CNG-Bc) and collateral-rich (CNG-B6) mice at 1, 5 and 24h after permanent middle cerebral artery occlusion (pMCAo). MRI-derived penumbra and ischemic core volumes were confirmed by histology in a subset of mice at 5 and 24h after pMCAo.

Correspondence: Yen-Yu Ian Shih, Ph.D. (shihy@unc.edu), Experimental Neuroimaging Laboratory, Departments of Neurology and Biomedical Research Imaging Center, 125 Mason Farm Road, CB# 7513, University of North Carolina, Chapel Hill, NC 27599, Tel: 919-843-4729, Fax: 919-843-4456; or James E Faber, Ph.D. (james_faber@med.unc.edu), Department of Cell Biology and Physiology, 6309A Medical Biomolecular Research Building, CBF# 7545, University of North Carolina, Chapel Hill, NC 27599, Tel: 919-966-0327.

*Y.C.J.K. and E.A.O. contributed equally to this work.

Conflict(s)-of-Interest/Disclosure

N/A

Results—Although perfusion deficit volumes were similar between strains 1h after pMCAo, diffusion deficit volumes were 32% smaller in collateral-rich mice. At 5h, collateral-rich mice had markedly restored perfusion patterns showing reduced perfusion deficit volumes, smaller infarct volumes, and smaller perfusion-diffusion mismatch volumes compared with the collateral-poor mice ($p<0.05$). At 24h, collateral-rich mice had 45% smaller T_2-weighted lesion volumes ($p<0.005$) than collateral-poor mice, with no difference in perfusion-diffusion mismatch volumes because of penumbral death occurring 5 to 24h after pMCAo in collateral-poor mice.

Conclusions—Variation in collateral extent significantly alters infarct volume expansion, transiently affects perfusion and diffusion MRI signatures, and impacts salvage of ischemic penumbra after stroke onset.

Keywords

magnet resonance imaging; perfusion; diffusion; collateral circulation; mouse

Subject Terms

Imaging and Diagnostic Testing (Magnetic Resonance Imaging (MRI)); Stroke (Ischemic Stroke); Genetics (Genetics)

Introduction

Collateral vessels are anastomoses that connect adjacent arterial trees and reroute perfusion around obstructed arteries or veins. Variation among individuals in the extent of native collaterals (i.e., number and/or diameter) may serve as a prognostic determinant of stroke severity and improve clinical risk-benefit decisions for treatment options.[1, 2] Angiographic studies grading collateral circulation in patients with acute stroke have found that final infarct size[3, 4] and functional outcome deficit vary inversely with collateral flow.[5–7] Patients with robust collateral circulation also have improved outcomes after tissue-type plasminogen activator (tPA) administration[4] (including reduced risk of hemorrhaging[8]) and/or intra-arterial revascularization,[9–11] suggesting that collateral extent significantly impacts the success of therapeutic interventions for acute ischemic stroke.

Imaging of perfusion in acute stroke patients using computed tomography (CT) or magnetic resonance imaging (MRI) is routine for accurate diagnosis and volumetric assessments of ischemic tissue. Contrast-enhanced CT,[3] MRI[12] and arterial spin-labeled perfusion MRI[13, 14] are also used clinically to differentiate hemorrhagic stroke and assess collateral status. Ischemic stroke registries that centrally store these data have been used retrospectively to examine how collateral circulation alters lesion evolution.[3, 7, 12, 15, 16] Such analyses consider many outcome-modifying variables (e.g., age, sex, co-morbidities, vascular risk factors, type/time of therapeutic intervention). However, they cannot account for all variables that contribute to acute stroke heterogeneity, resulting in conclusions based on correlation rather than causation. Recently, a novel mouse model has been developed that permits examination of the contribution of variation in collateral extent on variation in lesion progression, because genetic and environmental differences are controlled.[17] Two congenic (CNG) mouse lines were constructed that are isogenic except at a discrete locus on

chromosome 7, *Determinant of collateral extent-1* (*Dce1*), whose allelic variants determine 85% of the wide variation in collateral extent present in different inbred mouse strains: CNG-Bc are congenic wild-type BALB/cByJ (Bc) mice with sparse, small-diameter pial collaterals, while CNG-B6 are congenic Bc mice that harbor the C57BL/6J (B6) allele of *Dce1,* resulting in abundant, large-diameter collaterals. Because these mice differ only in collateral extent, they provide a unique opportunity to examine the role of collaterals, per se, on stroke progression.

In this study, congenic mice were subjected to pMCAo to determine how differences in collateral extent affect ischemic tissue evolution. We used perfusion, diffusion, and T_2-weighted MRI techniques that are commonly used to characterize ischemic core and estimate penumbra.[18–21] To more specifically assess the role of collaterals and exclude confounding reperfusion factors, we used MRI at 1, 5, and 24h after pMCAo. To corroborate the MR findings, we performed cleaved caspase-3 (CC3) and heme oxygenase-1 (HO-1) immunohistochemistry in a subset of animals to quantify ischemic core and penumbra, respectively. Additionally, we also used this unique dataset to derive specific MR apparent diffusion coefficient (ADC) and cerebral blood flow (CBF) deficit thresholds that best approximate histological ground truth. Compared with collateral-poor CNG-Bc mice, the collateral-rich CNG-B6 mice showed significantly smaller ADC deficit volume, CBF deficit volume, and more rescued penumbral tissue. Our data demonstrate that collateral extent is a key determinant of infarct evolution in mice and, if confirmed in humans, should be considered as an outcome-modifying variable in stroke clinical trials.

Materials and Methods

Animal Preparation

Two congenic mouse strains on the Bc background with distinct pial collateral extent profiles (Figure 1, see Introduction) were studied (n=22/strain, male, 3–4 months-age).[17] Following an overnight fast, mice were anesthetized with 1.5–2% isoflurane and their respective rectal temperature, blood O_2 saturation, and pulse/respiration rates were monitored using a MouseOx Plus (STARR Life Science Corp., Oakmont, PA) and maintained at 37±0.5°C, >97%, 380±10 bpm/100±10 bpm during surgery and scanning. A 2 mm aseptic craniotomy was performed and pMCAo was performed by cauterization at the M2-MCA level.[22] The craniotomy was closed with gelfoam (Pfizer Inc, 0009-0396-05, New York, NY) and dental cement to avoid susceptibility artifact during MR scans. After pMCAo mice were maintained in the scanner under 0.75–1% isoflurane delivered in 25% O_2 at a flowrate of 1 L/min. A subset of mice were scanned only once at either 1h (n=9/congenic strain), 5h or 24h (n=4/ congenic strain) after pMCAo for histological assessment. The remaining subjects underwent longitudinal scans. All studies were approved by the Institutional Animal Care and Use Committee of the University of North Carolina at Chapel Hill.

Magnetic Resonance Imaging Acquisition

MRI data were acquired using a Bruker BioSpec 9.4 Tesla system with a BGA-9S gradient insert (Bruker Corp., Billerica, MA). A home-made surface coil (with an internal diameter

of 0.8 cm) was used for brain imaging. For CBF measurement, an additional actively decoupled heart coil was used for continuous cardiac spin labeling (CSL).[23] This was achieved by a two-shot gradient-echo echo-planar imaging (EPI) sequence with bandwidth=300 kHz, TR/TE=3000/5 ms, labeling duration=2.524 s, post-labeling delay=300 ms, matrix=64x64, FOV=1.6x1.6 cm, 10 slices and slice thickness=0.75 mm. Diffusion-weighted images were acquired with the same geometry using two-shot spin-echo EPI with bandwidth=300 kHz, TR/TE=3000/22 ms, δ/Δ=4/12 ms, number of B_0=5, number of directions=30 and *b*-value=1200 s/mm^2. T_2-weighted anatomic images were acquired using a RARE sequence with spectral width=47 kHz, TR/TE=2500/44 ms, matrix=144x144, RARE factor=8, number of averages=20, FOV=1.44x1.44 cm, 10 slices and slice thickness=0.75 mm.

Histological Confirmation of the Ischemic Lesion

Because no reliable histological biomarker can delineate the border zone between penumbra and ischemic core within the first hour of stroke, stereological morphometric analysis was performed on a subset of mice at 5 and 24h after pMCAo (n=5/congenic strain/end point). Mice were euthanized by Euthasol overdose (100 mg/kg, i.p.) and transcardially perfused with 25 mL of 1x PBS (pH 7.2) followed by 25 mL of 4% PFA. Extracted brains were postfixed in 4% PFA overnight, followed by 30% sucrose until they sank and frozen to a chilled sliding microtome. Serial 30 μm-thick coronal sections were sliced between +2.2 mm anterior and −4.5 mm posterior of Bregma (as determined by atlas-derived landmarks), collecting only one of every 10 sections (21–23 sections/mouse/marker) for free floating immunohistochemistry. Sections were initially incubated in a MOM kit (PK-2200 Vector Laboratories, Burlingame, CA) according to the manufacturer's protocol or blocking solution (1% Bovine Serum Albumin, 0.4%Triton X-100 and 4% Normal Goat Serum in PBS) for 20 minutes to block non-specific binding. Sections were immunostained overnight at 4°C with either the penumbral marker mouse monoclonal antibody against heme oxygenase-1 (HO-1; 1:50, Enzo Life Science, ADI-OSA-110, Farmingdale, NY) or the ischemic core marker rabbit polyclonal antibody against cleaved caspase-3 (CC3; 1:100, Cell Signaling, 9661, Danvers, MA) and visualized with Alexa Fluor secondary antibodies (1:800; Molecular Probes, Carlsbad, CA). Volumes of ischemic core, penumbra and non-immunoreactive tissue were quantified stereologically using the Cavalieri estimator method on Stereo Investigator (v7.5; MBF Bioscience, Microbrightfield, Inc., Williston, VT) and corrected for dehydration-related shrinkage in slice thickness and edema using the 'indirect method'.[24] Systematic random samples were unbiasedly counted in 50 μm^2 frames within manually defined boundaries of each hemisphere using a 10 μm optical dissector with 2 μm upper and lower guard zones. Stereological imaging was performed with an Olympus BX50 microscope using a 60x 1.4 NA oil-immersion objective with a calculated coefficient of error of intra-animal variation of less than 0.1.

Data Processing and Analysis

Image analysis was performed using Statistical Parametric Mapping (SPM) in a custom-written Matlab (MathWorks Inc., Natick, MA) script.[25] Images were skull-stripped, co-registered across subjects and analyzed using established protocols that we published

previously.[26, 27] Specifically, CBF was calculated from CSL data using $CBF=\frac{(\lambda/T_1)(S_C-S_L)}{(S_L+(2\alpha-1)S_C)}$, where S_C and S_L are the MR signal intensities from the control and labeled images, respectively. λ is the water brain-blood partition coefficient, T_1 is that of tissue, and α is the arterial spin-labeling efficiency. For λ, T_1, and α we used 0.9, 1.9, and 0.7s, respectively.[28] Apparent diffusion coefficient (ADC) maps were calculated from the diffusion weighted images using $ADC=\frac{ln(S_0/S_1)}{(b_1-b_0)}$, where S_1 is the signal intensity obtained at b_1 (1200 s/mm^2) and S_0 is the signal intensity obtained at b_0 (0 s/mm^2). Group-averaged CBF, ADC, and T_2-weighted images for each experimental group and time-point were presented.

To better identify a specific ADC or CBF threshold reflecting histological measure, a range of ADC (0.45–0.6 mm^2/s) and CBF (0.175–0.35 ml/g/min) thresholds was used to compute their respective deficit volumes that underwent best-fit correlations with respect to histologically-defined volumes using an established method.[29] ADC and CBF deficit thresholds were calculated using Euclidean distances between true histologically-defined and threshold-dependent MRI volumes. Polynomial curves up to a degree of 4 were fitted to predict distances at unmeasured threshold values and the curve that best balanced over- and under-fitting the two volumes were selected as the optimal threshold cut-off for ADC and CBF deficits.

The values in the ipsilesional hemisphere were calculated based on the MR perfusion and diffusion deficits that delineated with our histologically guided thresholds, while the values in the contralesional hemisphere were measured with size-matched mirror-ROIs. T_2-weighted lesion volumes were quantified by thresholding hyper-intense signals (≥2 SD of contralateral normal cortical tissue) as described previously.[26] The ratio of MR-derived penumbral loss was defined as the difference in ADC deficit volumes between two time points divided by the mismatch volume at 1h.[15] The ratio of infarct growth was defined as the difference in ADC deficit volumes between the two time points divided by the T_2-weighted lesion volume at 24h.[15]

Statistical analysis was performed using SPSS software (IBM SPSS statistics 21, IBM Corp., Armonk, NY). To compare the difference in the deficit volumes between two congenic strains at multiple time points, unpaired two-way ANOVA followed by Tukey's HSD and Scheffe *post hoc* test was performed for data-passing and not-passing homogeneity test, respectively. Significant difference in ADC or CBF value, the ratio of penumbra tissue loss and the ratio of infarct growth between the two congenic strains at a particular time-point was assessed by a two-tailed independent t-test. All data in text are presented as mean ±SEM.

Results

Physiological parameters remained consistent throughout the MRI scans at 1, 5 and 24h after pMCAo. Beause no significant difference in CBF and ADC intensities or volumes were observed 24h after pMCAo within congenic mice that either received a single scan (n=4 per strain) or longitudinal scans (n=5 per strain in the cohort for 5h and 24h multiple scans), data collected for each time-point were compiled together for analysis. One CNG-Bc mouse was

excluded from the data because of a negative mismatch volume detected 5h after pMCAo, likely because of artifact during imaging acquisition. Figure 2 shows group-averaged CBF, ADC, and T_2-weighted images for each time-point in CNG-B6 (n=9 per time-point) and CNG-Bc mice (n=9 at 1 and 24h, n=8 at 5h) after pMCAo. By using a within-subject comparison with histological data, we identified ADC and CBF deficit thresholds of 0.541 mm^2/s and 0.255 ml/g/min after pMCAo best approximated the tissue deficit volume defined by CC3 (necrotic / apoptotic cells) and CC3+HO-1 (necrotic / apoptotic cells + penumbra) expression, respectively (Figure 3A,B). These thresholds were used for subsequent analyses. With these optimized thresholds, we also found significant correlations between ADC deficit and CC3 lesion volumes (Figure 3C) and also CBF deficit and CC3+HO-1 lesion volumes (Figure 3D).

At 1h after pMCAO we observed marked reductions in CBF values in the lesion side compared with the contralesional (normal) hemisphere as expected (Figure 4A). We observed no significant differences in the MR-derived CBF deficit volume at this time-point (Figure 5A). The mean ADC values were not different between the two groups, but ADC deficit volumes were significantly smaller in CNG-B6 (15.957±1.305 mm^3) than CNG-Bc (23.325±4.592 mm^3; $p<0.005$; Figure 5B). No significant difference in perfusion-diffusion mismatch volumes was found at 1h (16.562±6.817 mm^3 for CNG-B6 and 14.370±7.372 mm^3 for CNG-Bc; $p>0.05$; Figure 5C). Additionally, no differences were observed between congenic strains in T_2-weighted infarct volume at 1h (Figure 5C,D), likely because of the low sensitivity of this method to detect ischemic tissue during the hyperacute phase of pMCAo.

At 5h after pMCAo CBF deficit volumes were significantly reduced in collateral-rich CNG-B6 (19.692±5.208 mm^3) compared with collateral-poor CNG-Bc mice (32.425±8.213 mm^3; $p<0.005$; Figure 5A), suggesting significant restoration of tissue perfusion by collaterals. The mean ADC values were not different between the two groups, but ADC deficit volumes were significantly smaller in CNG-B6 (16.165±3.212 mm^3) than CNG-Bc (24.481±4.777; $p<0.005$; Figures 5B). A significantly smaller perfusion-diffusion mismatch in CNG-B6 was observed (3.528±2.596 mm^3 compared with 10.758±7.661 mm^3 in CNG-Bc; $p<0.05$; Figure 5C). The infarct volume defined by T_2-weighted images in CNG-B6 (9.876±1.883 mm^3) was also significantly smaller than CNG-Bc (16.327±3.516 mm^3; $p<0.005$; Figure 5D). No significant difference in the loss of perfusion-diffusion mismatch tissue (1.257±6.854 mm^3 for CNG-B6 and 8.047±11.754 mm^3 for CNG-Bc; $p>0.05$; Figure 6A), as well as the growth of T_2-weighted lesion volume (1.149±2.939 mm^3 for CNG-B6 and 3.484±5.089 mm^3 for CNG-Bc; $p>0.05$; Figure 6B), were found from 1 to 5h.

At 5h after pMCAo the CBF deficit volumes remained significantly reduced in collateral-rich CNG-B6 (19.370±5.179 mm^3) compared with those in collateral-poor CNG-Bc mice (32.021±8.957 mm^3; $p<0.005$; Figures 5A). The mean ADC values were not different between the two groups, but ADC deficit volumes were significantly smaller in CNG-B6 (17.379±5.945 mm^3) than CNG-Bc (28.713±3.6826 mm^3; $p<0.005$; Figures 5B). No significant difference in perfusion-diffusion mismatch volumes was found (1.473±1.245 mm^3 for CNG-B6 and 3.331±2.648 mm^3 for CNG-Bc; $p>0.05$; Figure 5C). The infarct volume defined by T_2-weighted images in CNG-B6 (18.133±4.231 mm^3) was significantly

smaller than CNG-Bc (33.527±3.829 mm^3; $p<0.005$; Figure 5D). In addition, loss of perfusion-diffusion mismatch tissue (approximate penumbra) from 5 to 24h became significantly different between CNG-B6 (6.532±7.697%) and CNG-Bc (36.376±8.289%). The growth of T_2-weighted lesion volume also differed between CNG-B6 (6.137±3.225%) and CNG-Bc (15.076±2.229%) (both $p<0.05$; Figures 6A,B).

Discussion

The present study sought to differentiate the contribution of variation in pial collateral circulation to the evolving perfusion and diffusion MRI signals within the first 24h after acute stroke. Using congenic mouse strains that differ solely in their collateral extent, we report that: (1) Genetic specification of “poor” versus “good” collaterals alters the initial ADC deficit volumes and the ability to salvage ‘at-risk’ tissue within 5h after stroke. (2) Although CBF deficit volume does not differ between the two congenic strains at 1h after pMCAo, collateral perfusion in collateral-rich mice is higher and sufficient to restrict expansion of initial ADC deficit volume. (3) Within 5h after pMCAo, collateral-rich mice display small CBF deficit volume, resulting in significant rescue of penumbra; while collateral-poor mice experience a larger area that remains at-risk, demonstrating that collateral extent plays a major role in altering the outcome of the second wave of cell death during permanent focal ischemia. (4) The imaging protocols and ADC/CBF thresholds established herein in mice demonstrate sufficient sensitivity and specificity to detect ischemic tissue evolution and thus offer a technical foundation for future studies investigating the efficacy of “collateral therapeutics”.

Wide variation in collateral extent among 21 inbred mouse strains is found to be tightly correlated with similarly wide variation in infarct volume after pMCAo and links to variants of the *Dce1* locus in these strains,[22, 30] suggesting that genetic polymorphisms underlying differences in collateral extent may be important risk factors for poor stroke outcome. However, other gene variants not associated with differences in collateral extent can also alter stroke severity, including the expression and activity of proteins that could affect infarct progression post-stroke. In addition, uncontrollable physiological differences between wild-type mouse trains, for instance, mean arterial pressure and immune response, might contribute to lesion evolution. The use of congenic mice with genetic variability restricted to a single locus shown to be the major determinant of anatomic variation in collaterals in mice allowed us to test for causation between collateral extent and the severity of the ischemic lesion and its evolution. To our knowledge, this is the first study to dissect the causal role of collateral extent, per se, in ischemic lesion evolution during the hyperacute, acute and early-chronic phases after pMCAo. Permanent MCAo in mice immediately reduces averaged CBF in the MCA territory by 50%,[31] and irreversibly results in necrotic death within minutes in regions where perfusion drops by ≥80%.[32] Permanent MCAo in both congenic lines resulted in significant reductions in CBF, yet mean CBF within perfusion deficit volumes were significantly greater in collateral-rich compared with collateral-poor mice 1h after stroke onset (40.69±4.31% and 38.23±2.05%, respectively) and reduced the initial ischemic core volume by 31.50% as defined by ADC deficit thresholds. This immediate retrograde collateral perfusion of the MCA territory is established within seconds after occlusion because of the large increase in cerebral perfusion pressure (CPP) across the collateral

network.[33, 34] Although mathematical models have predicted that pial collaterals can continue to maintain 15% of overall MCA baseline CBF immediately after pMCAo,[35] retrograde collateral perfusion to the proximal MCA territory is insufficient to preserve cellular function during this hyperacute phase, resulting in death for most cells in this region if CBF is not sufficiently restored.

At 5h after pMCAo, a significantly smaller CBF deficit volume was found in collateral-rich CNG-B6 mice compared with their collateral-poor counterparts. Studies in mice have shown that during the first few hours of collateral perfusion, presumed fluid shear stress-mediated dilation results in a 26% increase in collateral diameter after major vessel occlusion. Collaterals subsequently undergo outward remodeling of lumen diameter that requires 3–6 days, depending on genetic background, to achieve maximal remodeling (~2-to-4-fold increase in anatomic lumen diameter).[22] Changes in smooth muscle tone, plus the initial driving force of CPP across the collateral network induced by occlusion, are the primary determinants of collateral blood flow during the acute phase of pMCAo. However, further changes in collateral flow induced by alterations in CPP, such as those produced by downstream collapse of the venous network from insufficient inflow, will also impact delivery of oxygen to the territory at risk.[33, 36] The lack of change in ADC threshold volumes between 1 and 5h after pMCAo in collateral-rich mice, coupled with a significant reduction in perfusion-diffusion mismatch volume, indicates that collateral circulation can rescue penumbral tissue from death. On the other hand, in the collateral-poor mice, collateral flow is insufficient to prevent the second wave of cellular death resulting from an inability to restore adequate circulation to the entire MCA penumbral territory. Using the oxidative stress marker HO-1 expressed in penumbral tissue after pMCAo,[37] we found that mismatch of perfusion deficit volumes below 0.255 ml/g/min and diffusion deficit volumes below 0.541 mm^2/s accurately estimate penumbral volume in both congenic strains.

Infarct volume at 24h after pMCAo, as confirmed by ADC deficit volumes and T_2-weighted imaging, was significantly smaller in collateral-rich mice. The perfusion-diffusion mismatch volumes of both congenic strains were found to be less than 5 mm^3, which is consistent with the small penumbral volumes delineated by suppressed cerebral protein synthesis with preserved ATP production 8h after pMCAo in mice.[38] Our detection of a significant divergence of ADC and CBF deficit volumes between congenic strains demonstrates that collateral circulation dictates initial infarct size, infarct expansion, and whether penumbral tissue will be rescued. Multimodal MRI techniques are improving the efficiency of clinical stroke diagnosis and allow rapid estimation of penumbral tissue volume as early as the acute phase of ischemic stroke, which is important in balancing the risk versus benefit of reperfusion therapy.[39, 40] The controversy surrounding the use of perfusion-diffusion mismatch to indicate penumbra and the course of stroke treatment is in part attributed to the lack of consistency in defining deficit thresholds, overestimation of the tissue at risk, assumption of the irreversible diffusion lesions, and differences in the parameters used during acquisition.[40–42] Furthermore, the dynamic nature and heterogeneous distribution of the penumbra can cause significant fluctuations in perfusion and diffusion deficit volumes during acute stroke[43, 44]—variation that is only accentuated when collateral extent varies among subjects.[6, 7, 45] Our findings suggest caution to be taken when referring to the “penumbra” or “perfusion-diffusion mismatch volume” at a fixed time-point as a prognostic

or treatment criteria, without carefully considering the role of collateral circulation and the consequent temporal evolution of ischemic penumbra.

Mouse perfusion and diffusion MRI have many challenges, including strong susceptibility artifacts and lack of commercially available hardware for high-quality two-coil ASL.[23, 46, 47] More importantly, no “gold-standard” ADC and CBF thresholds exist for probing ischemic tissue in rodents. We addressed these problems herein by optimizing our thresholds against histologically-defined volumes, leading to a strategy for mapping the evolution of ischemic tissue in mice. One limitation of our study is that T_1 relaxation times increase after stroke and may result in decreased CBF signals.[48, 49] Thus, even though mismatch volumes in our study may better approximate penumbra volumes in mice with different collateral extents, they may not represent the absolute size of ischemic penumbra.

Conclusions

In summary, we performed quantitative perfusion and diffusion MRI in congenic mice differing in collateral extent to investigate the relationship between the ischemic penumbra and the vigor of the collateral circulation. Our findings using mice with identical genetic background but with congenically specified “good” versus “poor” collaterals demonstrate that the presence of good collaterals results in penumbral salvage within the first 5h of pMCAo followed by reduced perfusion-diffusion mismatch tissue loss during the 5–24h period. The results demonstrate the utility of this mouse model to explore the development of therapeutic strategies to enhance collateral perfusion post-stroke onset.[50] Additional studies combining this genetic mouse model with transient MCAo followed by post-labeling delays, will allow investigation of how reperfusion interacts with inherent differences in collateral circulation among individuals to determine the dynamic behavior of the ischemic penumbra.

Acknowledgments

Sources of Funding

EO is supported by National Heart, Lung, and Blood Institute training grant (T32HL069768). YYIS is supported by grants from National Institute of Neurological Disorders and Stroke (R01NS091236), National Institute of Mental Health (R01MH111429, R41 MH113252, R21MH106939), National Institute on Alcohol Abuse and Alcoholism (U01 AA020023, R01 AA025582), American Heart Association (15SDG23260025), and is an Ellen Schapiro & Gerald Axelbaum Investigator and Young Investigator Award recipient of the Brain & Behavior Research Foundation. National Institute of Neurological Disorders and Stroke (R01NS083633, JEF) provided partial support for this work.

References

1. Liebeskind DS. Collateral circulation. Stroke. 2003; 34:2279–2284. [PubMed: 12881609]
2. Shuaib A, Butcher K, Mohammad AA, Saqqur M, Liebeskind DS. Collateral blood vessels in acute ischaemic stroke: A potential therapeutic target. Lancet Neurol. 2011; 10:909–921. [PubMed: 21939900]
3. Kawano H, Bivard A, Lin L, Spratt NJ, Miteff F, Parsons MW, et al. Relationship between collateral status, contrast transit, and contrast density in acute ischemic stroke. Stroke. 2016; 47:742–749. [PubMed: 26839354]

4. Souza LC, Yoo AJ, Chaudhry ZA, Payabvash S, Kemmling A, Schaefer PW, et al. Malignant cta collateral profile is highly specific for large admission dwi infarct core and poor outcome in acute stroke. AJNR Am J Neuroradiol. 2012; 33:1331–1336. [PubMed: 22383238]
5. Frolich AM, Wolff SL, Psychogios MN, Klotz E, Schramm R, Wasser K, et al. Time-resolved assessment of collateral flow using 4d ct angiography in large-vessel occlusion stroke. Eur Radiol. 2014; 24:390–396. [PubMed: 24078013]
6. Maas MB, Lev MH, Ay H, Singhal AB, Greer DM, Smith WS, et al. Collateral vessels on ct angiography predict outcome in acute ischemic stroke. Stroke. 2009; 40:3001–3005. [PubMed: 19590055]
7. Miteff F, Levi CR, Bateman GA, Spratt N, McElduff P, Parsons MW. The independent predictive utility of computed tomography angiographic collateral status in acute ischaemic stroke. Brain. 2009; 132:2231–2238. [PubMed: 19509116]
8. Bang OY, Saver JL, Kim SJ, Kim GM, Chung CS, Ovbiagele B, et al. Collateral flow averts hemorrhagic transformation after endovascular therapy for acute ischemic stroke. Stroke. 2011; 42:2235–2239. [PubMed: 21737798]
9. Bang OY, Saver JL, Kim SJ, Kim GM, Chung CS, Ovbiagele B, et al. Collateral flow predicts response to endovascular therapy for acute ischemic stroke. Stroke. 2011; 42:693–699. [PubMed: 21233472]
10. Marks MP, Lansberg MG, Mlynash M, Olivot JM, Straka M, Kemp S, et al. Effect of collateral blood flow on patients undergoing endovascular therapy for acute ischemic stroke. Stroke. 2014; 45:1035–1039. [PubMed: 24569816]
11. Ribo M, Flores A, Rubiera M, Pagola J, Sargento-Freitas J, Rodriguez-Luna D, et al. Extending the time window for endovascular procedures according to collateral pial circulation. Stroke. 2011; 42:3465–3469. [PubMed: 21960574]
12. Campbell BC, Christensen S, Tress BM, Churilov L, Desmond PM, Parsons MW, et al. Failure of collateral blood flow is associated with infarct growth in ischemic stroke. J Cereb Blood Flow Metab. 2013; 33:1168–1172. [PubMed: 23652626]
13. Wang DJ, Alger JR, Qiao JX, Gunther M, Pope WB, Saver JL, et al. Multi-delay multi-parametric arterial spin-labeled perfusion mri in acute ischemic stroke - comparison with dynamic susceptibility contrast enhanced perfusion imaging. Neuroimage Clin. 2013; 3:1–7. [PubMed: 24159561]
14. Yu S, Liebeskind DS, Dua S, Wilhalme H, Elashoff D, Qiao XJ, et al. Postischemic hyperperfusion on arterial spin labeled perfusion mri is linked to hemorrhagic transformation in stroke. J Cereb Blood Flow Metab. 2015; 35:630–637. [PubMed: 25564233]
15. Jung S, Gilgen M, Slotboom J, El-Koussy M, Zubler C, Kiefer C, et al. Factors that determine penumbral tissue loss in acute ischaemic stroke. Brain. 2013; 136:3554–3560. [PubMed: 24065722]
16. Cortijo E, Calleja AI, Garcia-Bermejo P, Mulero P, Perez-Fernandez S, Reyes J, et al. Relative cerebral blood volume as a marker of durable tissue-at-risk viability in hyperacute ischemic stroke. Stroke. 2014; 45:113–118. [PubMed: 24281229]
17. Sealock R, Zhang H, Lucitti JL, Moore SM, Faber JE. Congenic fine-mapping identifies a major causal locus for variation in the native collateral circulation and ischemic injury in brain and lower extremity. Circ Res. 2014; 114:660–671. [PubMed: 24300334]
18. Bouts MJ, Tiebosch IA, van der Toorn A, Hendrikse J, Dijkhuizen RM. Lesion development and reperfusion benefit in relation to vascular occlusion patterns after embolic stroke in rats. J Cereb Blood Flow Metab. 2014; 34:332–338. [PubMed: 24301289]
19. Leoni RF, Paiva FF, Kang BT, Henning EC, Nascimento GC, Tannus A, et al. Arterial spin labeling measurements of cerebral perfusion territories in experimental ischemic stroke. Transl Stroke Res. 2012; 3:44–55. [PubMed: 24323754]
20. Shen Q, Duong TQ. Magnetic resonance imaging of cerebral blood flow in animal stroke models. Brain Circ. 2016; 2:20–27. [PubMed: 26998527]
21. Tuor UI, Qiao M, Sule M, Morgunov M, Foniok T. Magnetic resonance imaging of ischemic injury produced by varying severities of photothrombosis differs in neonatal and adult brain. NMR Biomed. 2016

22. Zhang H, Prabhakar P, Sealock R, Faber JE. Wide genetic variation in the native pial collateral circulation is a major determinant of variation in severity of stroke. J Cereb Blood Flow Metab. 2010; 30:923–934. [PubMed: 20125182]
23. Muir ER, Shen Q, Duong TQ. Cerebral blood flow mri in mice using the cardiac-spin-labeling technique. Magn Reson Med. 2008; 60:744–748. [PubMed: 18727091]
24. Lin TN, He YY, Wu G, Khan M, Hsu CY. Effect of brain edema on infarct volume in a focal cerebral ischemia model in rats. Stroke. 1993; 24:117–121. [PubMed: 8418534]
25. Shih YY, Chen YY, Chen CC, Chen JC, Chang C, Jaw FS. Whole-brain functional magnetic resonance imaging mapping of acute nociceptive responses induced by formalin in rats using atlas registration-based event-related analysis. J Neurosci Res. 2008; 86:1801–1811. [PubMed: 18293420]
26. Kao YC, Li W, Lai HY, Oyarzabal EA, Lin W, Shih YY. Dynamic perfusion and diffusion mri of cortical spreading depolarization in photothrombotic ischemia. Neurobiol Dis. 2014; 71:131–139. [PubMed: 25066776]
27. Shih YY, Huang S, Chen YY, Lai HY, Kao YC, Du F, et al. Imaging neurovascular function and functional recovery after stroke in the rat striatum using forepaw stimulation. J Cereb Blood Flow Metab. 2014; 34:1483–1492. [PubMed: 24917039]
28. Shih YY, Wey HY, De La Garza BH, Duong TQ. Striatal and cortical bold, blood flow, blood volume, oxygen consumption, and glucose consumption changes in noxious forepaw electrical stimulation. J Cereb Blood Flow Metab. 2011; 31:832–841. [PubMed: 20940730]
29. Jacobs MA, Knight RA, Soltanian-Zadeh H, Zheng ZG, Goussev AV, Peck DJ, et al. Unsupervised segmentation of multiparameter mri in experimental cerebral ischemia with comparison to t2, diffusion, and adc mri parameters and histopathological validation. J Magn Reson Imaging. 2000; 11:425–437. [PubMed: 10767072]
30. Keum S, Lee HK, Chu PL, Kan MJ, Huang MN, Gallione CJ, et al. Natural genetic variation of integrin alpha l (itgal) modulates ischemic brain injury in stroke. PLoS Genet. 2013; 9:e1003807. [PubMed: 24130503]
31. van Dorsten FA, Hata R, Maeda K, Franke C, Eis M, Hossmann KA, et al. Diffusion- and perfusion-weighted mr imaging of transient focal cerebral ischaemia in mice. NMR Biomed. 1999; 12:525–534. [PubMed: 10668045]
32. Hossmann KA. Pathophysiology and therapy of experimental stroke. Cell Mol Neurobiol. 2006; 26:1057–1083. [PubMed: 16710759]
33. Pranevicius O, Pranevicius M, Pranevicius H, Liebeskind DS. Transition to collateral flow after arterial occlusion predisposes to cerebral venous steal. Stroke. 2012; 43:575–579. [PubMed: 22246692]
34. Winship IR, Armitage GA, Ramakrishnan G, Dong B, Todd KG, Shuaib A. Augmenting collateral blood flow during ischemic stroke via transient aortic occlusion. J Cereb Blood Flow Metab. 2014; 34:61–71. [PubMed: 24045399]
35. Ursino M, Giannessi M. A model of cerebrovascular reactivity including the circle of willis and cortical anastomoses. Ann Biomed Eng. 2010; 38:955–974. [PubMed: 20094916]
36. Defazio RA, Zhao W, Deng X, Obenaus A, Ginsberg MD. Albumin therapy enhances collateral perfusion after laser-induced middle cerebral artery branch occlusion: A laser speckle contrast flow study. J Cereb Blood Flow Metab. 2012; 32:2012–2022. [PubMed: 22781334]
37. Chen L, Wang L, Zhang X, Cui L, Xing Y, Dong L, et al. The protection by octreotide against experimental ischemic stroke: Up-regulated transcription factor nrf2, ho-1 and down-regulated nf-kappab expression. Brain Res. 2012; 1475:80–87. [PubMed: 22885292]
38. Hata R, Maeda K, Hermann D, Mies G, Hossmann KA. Dynamics of regional brain metabolism and gene expression after middle cerebral artery occlusion in mice. J Cereb Blood Flow Metab. 2000; 20:306–315. [PubMed: 10698068]
39. Heiss WD. Ischemic penumbra: Evidence from functional imaging in man. J Cereb Blood Flow Metab. 2000; 20:1276–1293. [PubMed: 10994849]
40. Sanelli PC, Sykes JB, Ford AL, Lee JM, Vo KD, Hallam DK. Imaging and treatment of patients with acute stroke: An evidence-based review. AJNR Am J Neuroradiol. 2014; 35:1045–1051. [PubMed: 23598836]

41. Kidwell CS, Jahan R, Gornbein J, Alger JR, Nenov V, Ajani Z, et al. A trial of imaging selection and endovascular treatment for ischemic stroke. N Engl J Med. 2013; 368:914–923. [PubMed: 23394476]
42. Nagakane Y, Christensen S, Ogata T, Churilov L, Ma H, Parsons MW, et al. Moving beyond a single perfusion threshold to define penumbra: A novel probabilistic mismatch definition. Stroke. 2012; 43:1548–1555. [PubMed: 22499579]
43. del Zoppo GJ, Sharp FR, Heiss WD, Albers GW. Heterogeneity in the penumbra. J Cereb Blood Flow Metab. 2011; 31:1836–1851. [PubMed: 21731034]
44. Ma H, Zavala JA, Teoh H, Churilov L, Gunawan M, Ly J, et al. Fragmentation of the classical magnetic resonance mismatch “penumbral” pattern with time. Stroke. 2009; 40:3752–3757. [PubMed: 19850896]
45. Christoforidis GA, Karakasis C, Mohammad Y, Caragine LP, Yang M, Slivka AP. Predictors of hemorrhage following intra-arterial thrombolysis for acute ischemic stroke: The role of pial collateral formation. AJNR Am J Neuroradiol. 2009; 30:165–170. [PubMed: 18768718]
46. Adamczak JM, Farr TD, Seehafer JU, Kalthoff D, Hoehn M. High field bold response to forepaw stimulation in the mouse. Neuroimage. 2010; 51:704–712. [PubMed: 20211267]
47. Bosshard SC, Baltes C, Wyss MT, Mueggler T, Weber B, Rudin M. Assessment of brain responses to innocuous and noxious electrical forepaw stimulation in mice using bold fmri. Pain. 2010; 151:655–663. [PubMed: 20851520]
48. van Dorsten FA, Olah L, Schwindt W, Grune M, Uhlenkuken U, Pillekamp F, et al. Dynamic changes of adc, perfusion, and nmr relaxation parameters in transient focal ischemia of rat brain. Magn Reson Med. 2002; 47:97–104. [PubMed: 11754448]
49. Hoehn-Berlage M, Eis M, Back T, Kohno K, Yamashita K. Changes of relaxation times (t1, t2) and apparent diffusion coefficient after permanent middle cerebral artery occlusion in the rat: Temporal evolution, regional extent, and comparison with histology. Magn Reson Med. 1995; 34:824–834. [PubMed: 8598809]
50. Ginsberg MD. Expanding the concept of neuroprotection for acute ischemic stroke: The pivotal roles of reperfusion and the collateral circulation. Prog Neurobiol. 2016; 145–146:46–77.

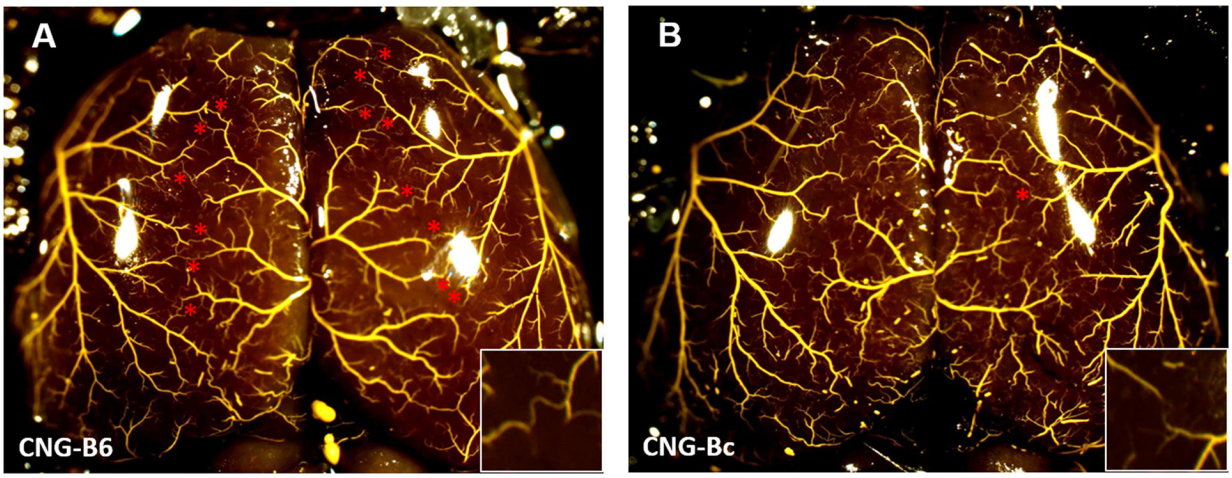

Figure 1. Genetic model of abundant versus sparse collaterals: congenic-B6 and congenic-Bc mice

Maximally dilated pre-capillary vessels filled with Microfil shows larger collateral number in congenic (CNG)-B6 compared to CNG5-Bc. Stars, MCA-to-ACA collaterals. Inset, higher magnification showing presence and absence of pial collaterals in watershed zone. CNG-Bc, congenic-line5 wildtype BALB/cByJ mice (2±1 MCA-to-ACA collaterals of 12±13 μm lumen diameter); CNG-B6, congenic-line5 wildtype BALB/cByJ mice with C57BL/6J *Dce1* genetic locus introgressed into genome (14±1 MCA-to-ACA collaterals of 20±2 μm diameter).[17]

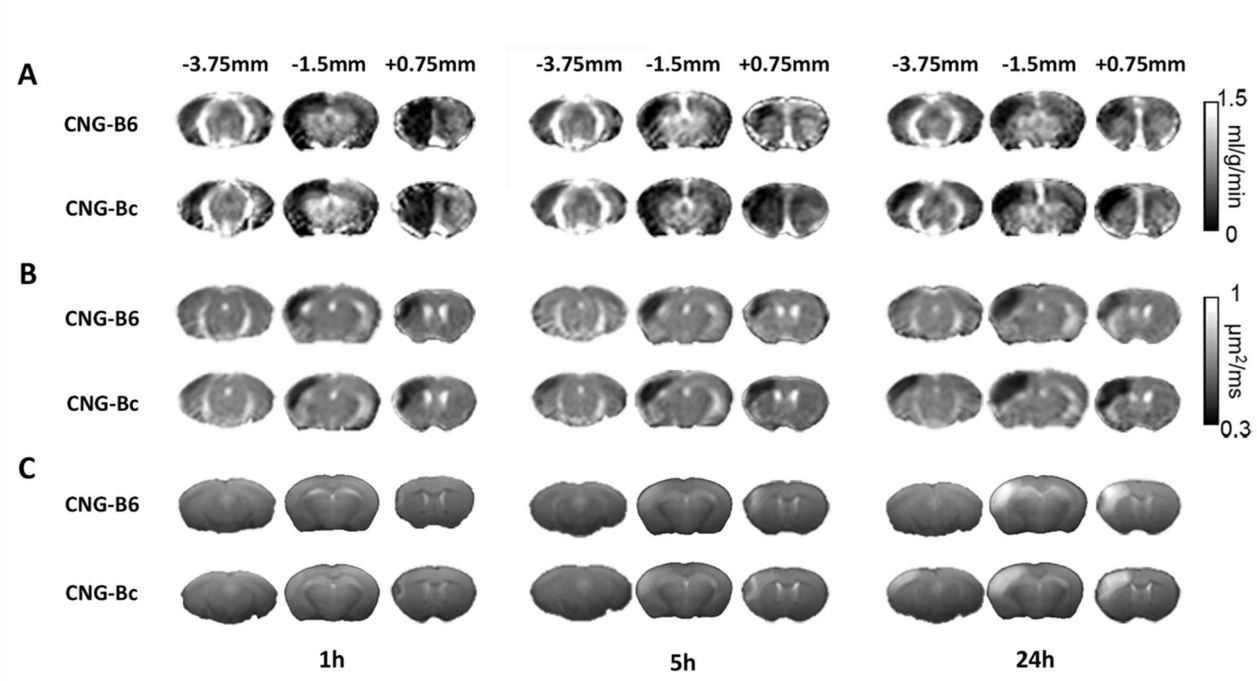

Figure 2. Perfusion and diffusion MRI and T2-weighted images in CNG-B6 and CNG-Bc mice after permanent MCAo (pMCAo)

Group-averaged CBF map (A), ADC map (B), and T2-weighted images (C) at 1, 5 and 24 h after pMCAo. Hypoperfused area was observed in the entire ipsilesional cortex at 1 h in both CNG-B6 and CNG-Bc mice. After 24 h, larger CBF, ADC deficit and final infarct area evident in anterior and posterior cortical regions in CNG-Bc.

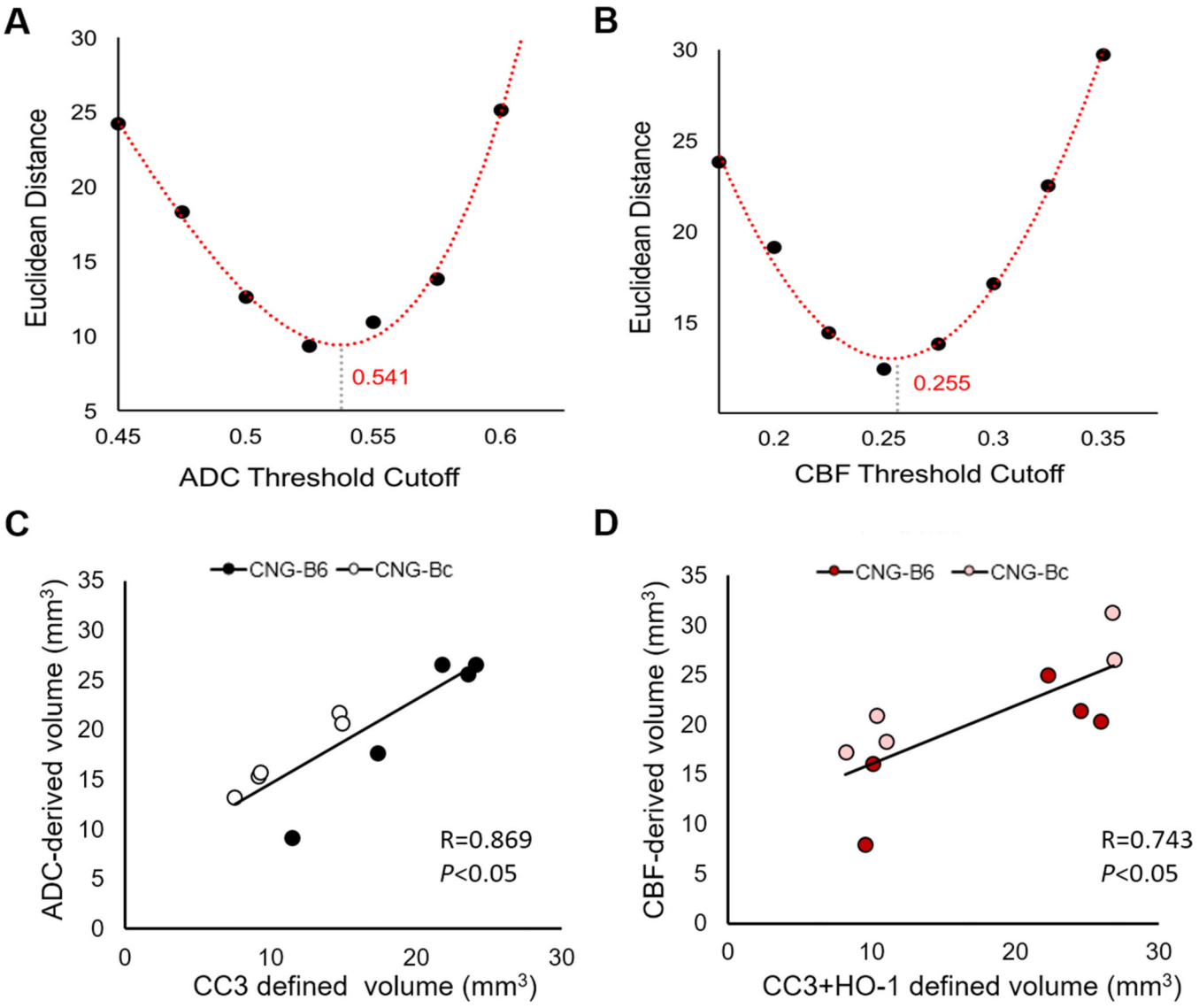

Figure 3. Lesion volumes defined by histological staining and comparison with MRI (C,D)

Optimal threshold of ADC- (A) and CBF-derived (B) lesion volumes based on the curve fitting. Histological staining: cleaved caspace3 (CC3), heme oxygenase-1 (HO-1).

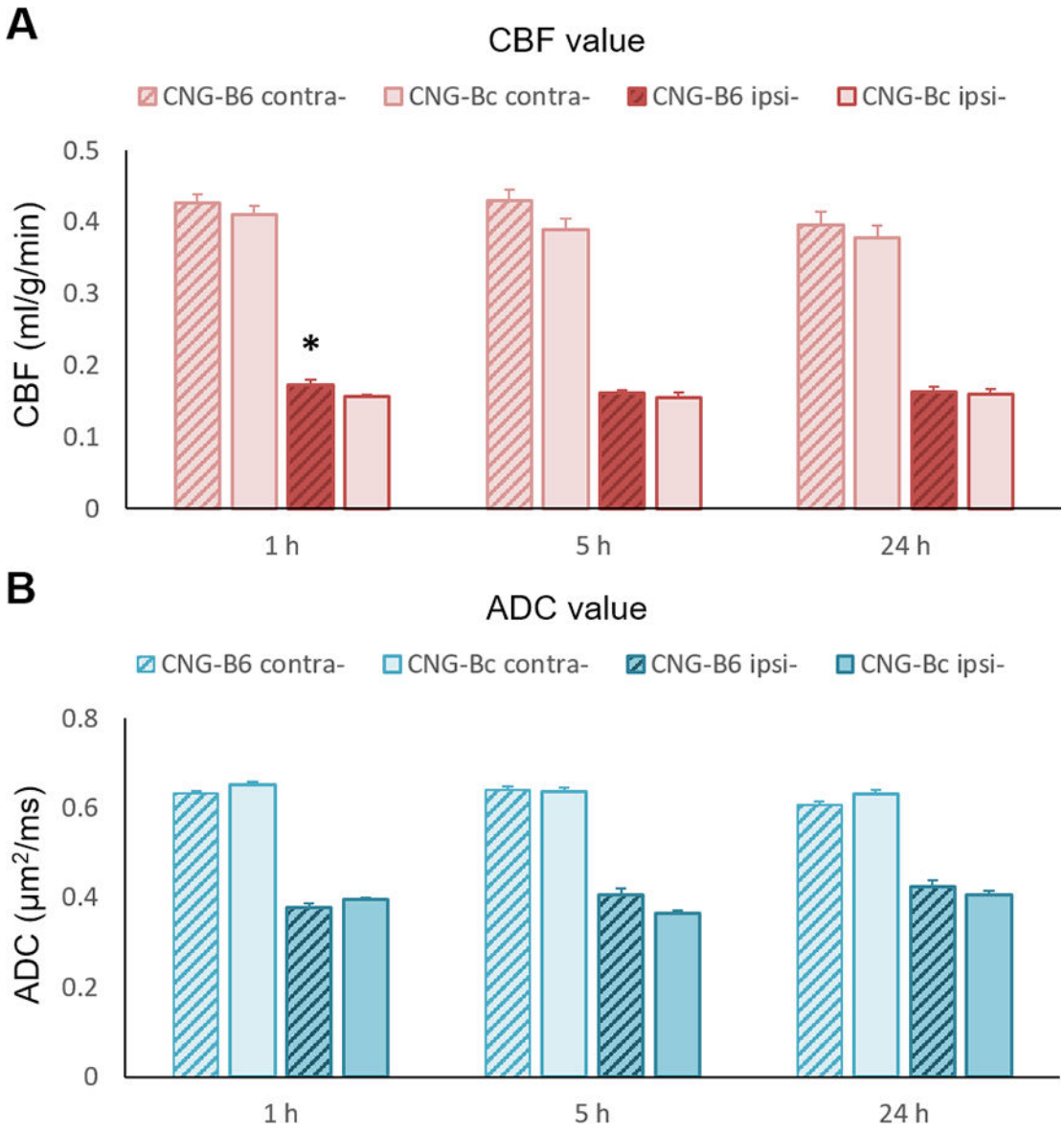

Figure 4. CBF and ADC values in CNG-B6 and CNG-Bc mice

(A) CBF and (B) ADC values in corresponding lesion volume at 1, 5 and 24 h after pMCAo. No significant change in CBF or ADC in contralesional hemisphere in both strains. Significantly higher CBF present in lesion area in CNG-B6 1h after pMCAo. Mean±SEM; *p<0.05 versus CNG-Bc.

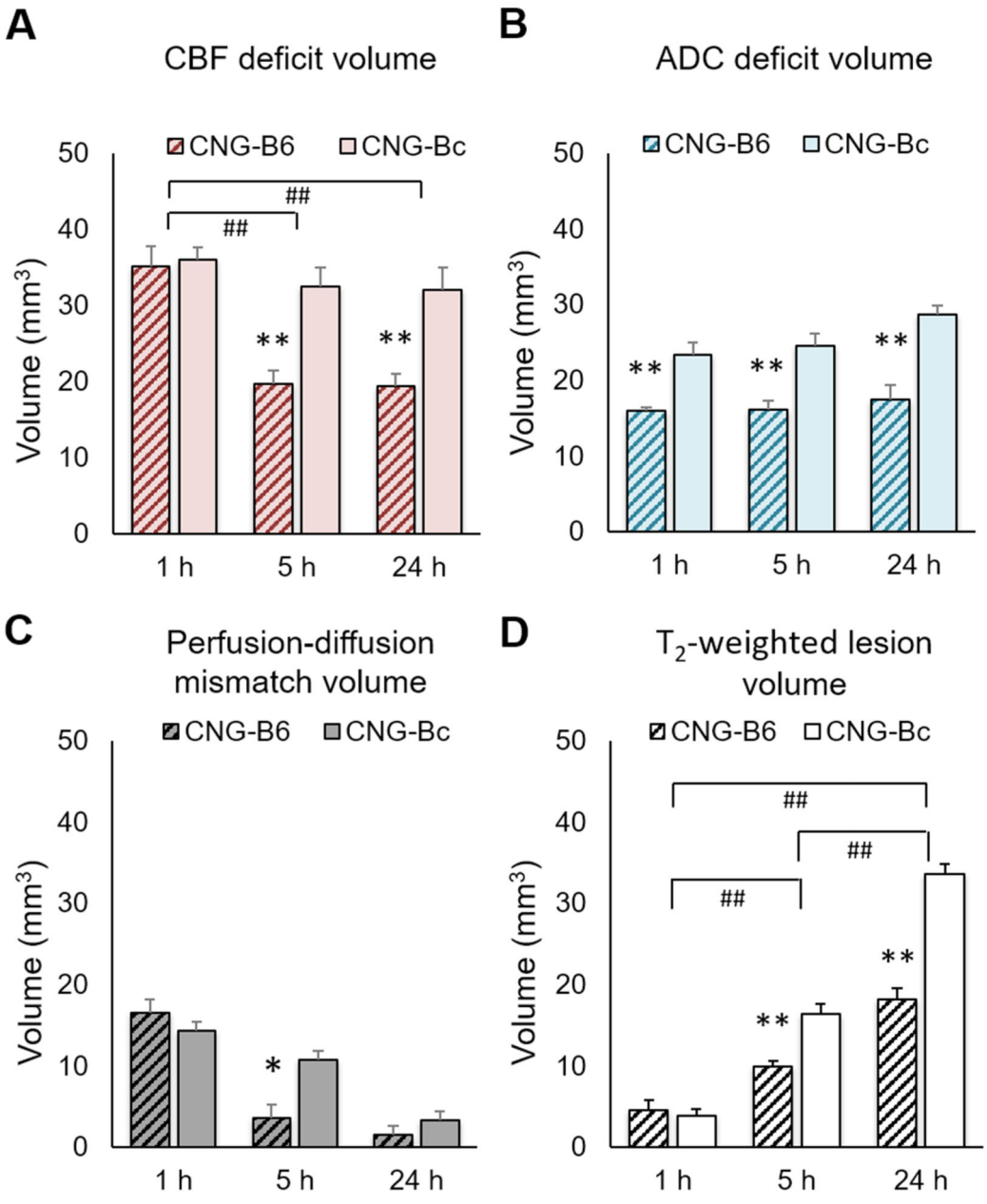

Figure 5. CNG-B6 mice shows smaller CBF deficit, ADC deficit, mismatch and T_2-weighted lesion volumes after pMCAo

Mean±SEM; *,**p<0.05,<0.005 versus CNG-Bc; #,##p<0.05,<0.005 versus time.

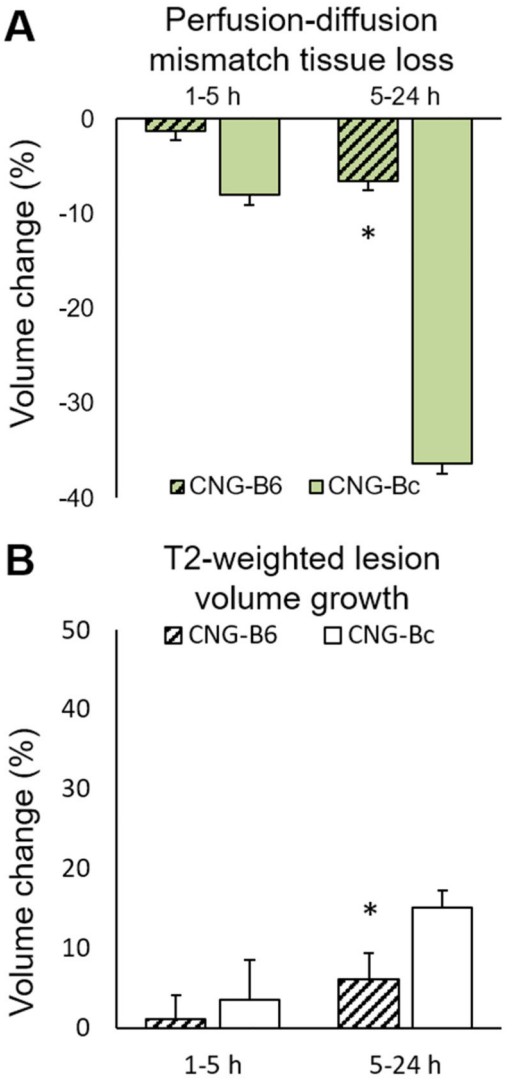

Figure 6. CNG-B6 shows smaller perfusion-diffusion mismatch tissue loss and T_2-weighted lesion volume growth after pMCAo

Mean±SEM; *p<0.05 versus CNG-Bc.